A new approach to measure the volume scattering function

Hiroyuki Tan,[1,*] Roland Doerffer,[1] Tomohiko Oishi,[2] and Akihiko Tanaka[2]

[1]*Institute for Coastal Research, Helmholtz-Zentrum Geesthacht, Center for Materials and Coastal Research, Max-Planck Strasse 1, D-21502 Geesthacht, Germany*

[2]*School of Marine Science and Technology, Tokai University, Orido 3-20-1, Shimizu-ku, Shizuoka-city, Japan*

** Hiroyuki.Tan@hzg.de*

Abstract: We present a novel optical approach to measure the volume scattering function (VSF) by image detection. The instrument design, based upon a combination of two reflectors, uses a unique measurement principle and allows the rapid simultaneous determination of scattering at a wide range of angles. The advantages of the newly developed scattering meter are that: 1) it can determine the scattering function from 8° to 172° at 1° intervals without changing the sensitivity of the detector, without moving any optical parts, and can do so within a few seconds, 2) the unique optical design facilitates determination of the spectral VSF over the full visible spectrum, i.e. it can obtain the VSF at a specific wavelength with an optional wavelength-resolution. Measurements under controlled conditions for the assessment of the instrument agreed well with theoretically predicted scattering functions. Measurements with cultured phytoplankton of different species revealed a significant variety of the VSF together with spectral variation. The observed results will stimulate and improve radiative transfer and/or two-flow models of light in the ocean, which is an important role for ocean color remote sensing algorithm development, particularly for coastal regions.

OCIS codes: (010.4450) Oceanic optics; (120.4640) Optical instruments; (120.5820) Scattering measurements; (010.1350) Backscattering.

Reference and links

1. R. W. Preisendorfer, "Application of radiative transfer theory to light measurement in the sea," Union Geod. Geophys. Inst. Monogr. **10**, 11–30 (1961).
2. E. Aas, "Two-stream irradiance model for deep waters," Appl. Opt. **26**(11), 2095–2101 (1987).
3. A. Morel, "Light and marine photosynthesis: a spectral model with geochemical and climatological implications," Prog. Oceanogr. **26**(3), 263–306 (1991).
4. R. Doerffer and J. Fischer, "Concentration of chlorophyll, suspended matter, and gelbstoff in case II water derived from satellite coastal zone color scatter data with inverse modeling methods," J. Geophys. Res. **99**(C4), 7457–7466 (1994).
5. J. E. Tyler and W. H. Richardson, "Nephelometer for the measurement of volume scattering in situ," J. Opt. Soc. Am. **48**(5), 354–357 (1958).
6. N. G. Jerlov, "Distribution of suspended material in the Adriatic sea," Arch. Oceanogr. Limnol. **11**, 227–250 (1958).
7. N. Højerslev, "Tydall and fluorescence measurements in Danish and Norwegian waters related to dynamical features," Rep. Inst. Phys. Oceanogr. Univ. Copenhagen **16** (1971).
8. T. J. Petzold, "Volume scattering functions for selected ocean waters," Tech. Rep. SIO **72–78**, Scripps Institution of Oceanography, San Diego, Calif. (1972).
9. E. Aas, "The calibration of a scatterance and fluorescence meter," Rep. Dept. Geophys. Univ. Oslo. **40** (1979).
10. R. Reuter, "Characterization of marine particles suspensions by light scattering (II). Experimental results," Oceanol. Acta **3**, 325–332 (1980).
11. J. R. V. Zaneveld, S. Pegau, and J. L. Mueller, "Volume scattering function and backscattering coefficients: instruments, characterization, field measurements and data analysis protocols," In J. L Mueller, G. S. Fargion & C. R. McClain (Eds.), Ocean optics protocols for satellite ocean color sensor validation, revision 4, Vol. IV:

#191692 - $15.00 USD Received 3 Jun 2013; revised 2 Jul 2013; accepted 8 Jul 2013; published 30 Jul 2013

Inherent optical properties: instruments, characterization, field measurements and data analysis protocols, NASA Tech. Memo. 2003–211621/Rev4-Vol.IV. Greenbelt: NASA Goddard Space Flight Center, 65–76 (2003).
12. X. Zhang, M. Lewis, M. Lee, B. Johnson, and G. Korotaev, "The volume scattering function of natural bubble populations," Limnol. Oceanogr. **47**(5), 1273–1282 (2002).
13. M. E. Lee and M. R. Lewis, "A new method of the measurement of the optical volume scattering function in the upper ocean," J. Atmos. Ocean. Technol. **20**(4), 563–571 (2003).
14. J. K. Lotsberg, E. Marken, J. J. Stamnes, S. R. Erga, K. Aursland, and C. Olseng, "Laboratory measurement of light scattering from marine particles," Limnol. Oceanogr. **5**, 34–40 (2007).
15. J. T. O. Kirk, "Point-source integrating-cavity absorption meter: theoretical principles and numerical modeling," Appl. Opt. **36**(24), 6123–6128 (1997).
16. R. Röttgers and R. Doerffer, "Measurements of optical absorption by chromophoric dissolved organic matter using a point-source integrating-cavity absorption meter," Limnol. Oceanogr. Methods **5**, 126–135 (2007).
17. G. Kullenberg, "Scattering of light by Sargasso sea water," Deep-Sea Res. **15**, 423–432 (1968).
18. H. Volten, J. F. Haan, J. W. Hovenier, R. Schreurs, W. Vassen, A. G. Dekker, H. J. Hoogenboom, F. Charlton, and R. Wouts, "Laboratory measurement of angular distributions of light scattered by phytoplankton and silt," Limnol. Oceanogr. **43**(6), 1180–1197 (1998).
19. X. Zhang, M. Lewis, and B. Johnson, "Influence of bubbles on scattering of light in the ocean," Appl. Opt. **37**(27), 6525–6536 (1998).
20. M. Chami, E. B. Shybanov, T. Y. Churilova, G. A. Khomenko, M. E.-G. Lee, O. V. Martynov, G. A. Berseneva, and G. K. Korotaev, "Optical properties of the particles in the Crimea coastal waters (Black Sea)," J. Geophys. Res. **110**, C11020 (2005), doi:10. 1029/2005JC003008.
21. T. Oishi, "Light scattering and polarization by suspended particulate matter in sea water," Rep. Inst. Phys. Oceanogr. Univ. Copenhagen **49** (1987).
22. A. Morel, "Diffusion de la lumière par les eaux de mer; résultats expérimentaux et approche théorique," in *Optics of the sea: NATO AGARD Lect. Ser.* **61**, (1973).
23. N. G. Jerlov, *Marine Optics* (Elsevier, Amsterdam, 1976).
24. R. M. Pope and E. S. Fry, "Absorption spectrum (380-700 nm) of pure water. II. Integrating cavity measurements," Appl. Opt. **36**(33), 8710–8723 (1997).
25. A. Morel, "Optical properties of pure water and pure sea water," in *Optical Aspects of Oceanography*, N.G. Jerlov and E.S. Nielson, eds. (Academic, New York, 1974), pp. 1–24.
26. W. E. Vargas and G. A. Niklasson, "Generalized method for evaluating scattering parameters used in radiative transfer models," J. Opt. Soc. Am. A **14**(9), 2243–2252 (1997).
27. K. Alexandra, B. Marcus, and D. Claus-Dieter, *COASTAL PHYTOPLANKTON: Photo guide for northern European seas* (Pfeil, München, 2010).
28. Alfred Wegener Institute for Polar and Marine Research (AWI), Biodiversity data provider, *http://planktonnet.awi.de*
29. D. T. Thomas, "Scattering by plasma and dielectric bodies," Ph.D. Thesis, Ohio State Univ., (1962).
30. E. Aas, "The refractive index of phytoplankton," Rep. Dept. Geophys. Univ. Oslo **46**, (1981).
31. E. Aas, "Refractive index of phytoplankton derived from its metabolite composition," J. Plankton Res. **18**(12), 2223–2249 (1996).
32. H. C. van de Hulst, *Light scattering by small particles* (Wiley, New York, 1957).
33. M. I. Mishchenko, J. W. Hovenier, and L. D. Travis, *Light scattering by nonspherical particles: theory, measurements, and applications* (Academic press, San Diego, 2000).
34. R. J. Gibbs, "Light scattering from particles of different shapes," J. Geophys. Res. **83**(C1), 501–502 (1978).
35. A. J. A. Smith, "The scattering of light by non-spherical particles," Rep. Dept. Geophys. Univ. Oxford, (2008).
36. D. Stramski, E. Boss, D. Bogucki, and K. J. Voss, "The role of seawater constituents in light backscattering in the ocean," Prog. Oceanogr. **61**(1), 27–56 (2004).
37. W. Zhou, G. Wang, Z. Sun, W. Cao, Z. Xu, S. Hu, and J. Zhao, "Variations in the optical scattering properties of phytoplankton cultures," Opt. Express **20**(10), 11189–11206 (2012).

1. Introduction

The spectral and angular distribution of the light scattering coefficient, i.e. the spectral volume scattering function (VSF), is defined as the dispersion of light in all directions from an infinitesimal scattering volume. The VSF and the absorption coefficient, both inherent optical properties (IOPs) of a medium, play a fundamental role in optical oceanography by determining the light field in aquatic media, as well as the water leaving radiant energy to the atmosphere crossing the sea surface. From the ocean color remote sensing perspective, for instance, they are vital parameters for solving the radiative transfer equation [1] and/or two-flow models [2], for obtaining information on primary production (e.g [3].), and for determining spatial distributions of specific water constituent concentrations in the upper-layer of the ocean (e.g. chlorophyll-a, yellow substance and suspending matters) [4] from satellites.

#191692 - $15.00 USD Received 3 Jun 2013; revised 2 Jul 2013; accepted 8 Jul 2013; published 30 Jul 2013

A typical measurement principle for VSF determination, which dates back to 1950s-1980s [5–10], is that either an optical sensor or a light projector turns around the center of the scattering volume. This principle has been used and advanced by several investigators. For instance, Zaneveld et al. [11] improved the basic method by mounting different sensors at several discrete scattering angles. However, this setup requires additional delicate calibrations between sensors. Zhang et al., Lee and Lewis, and Lotsberg et al. [12–14] presented a more advanced VSF meter with improved angular resolution. However, fundamental problems affecting VSF measurement, described below, remained.

Light absorption and attenuation (the sum of scattering and absorption) have been routinely measured in situ [e.g 15, 16], whereas the VSF is rarely measured [8, 13, 17] due to complicated measurement geometries and the difficulty of accurate measurements at forward and backward scattering angles. One problem is the large dynamic range of the scattering coefficient over all scattering angles that reaches typically 5 or 6 orders of magnitude. Furthermore, even in controlled laboratory scattering measurements, it is difficult 1) to prevent specular reflections of the primary light beam at physical boundaries [18], 2) to keep the particles in suspension during the measurement, 3) to avoid bubbles [12, 19], and 4) to perform accurate calibrations. As a consequence, instruments for VSF measurements became very complicated in their mechanical design. The measurements are typically quite time-consuming, determining scattering step by step over the entire range of angles [14], and the spectral resolution is often limited to one or only several wavelengths [20]. The spectral distribution of the VSF for particulate suspended matter is still mostly unknown due to the lack of direct measurement.

Here, we describe a novel optical design with an imaging detector that can acquire the VSF from 8° to 172° with a resolution of 1° in a few seconds. The instrument allows VSF measurements without changing the sensitivity of the detector and without any moving optical parts. Measurements in the visible spectral region from 400 nm to 700 nm at 20 nm intervals (10 nm steps from 680 nm to 700 nm) can be performed within 30 min. We present the characteristics of full spectral VSFs of some phytoplankton species.

2. Instrumentation

Background

The VSF, $\beta(\theta)$, is defined as the scattered radiant intensity oriented into a given scattering angle of θ, $I(\theta)$, per unit irradiance E and per unit of the infinitesimal scattering volume V:

$$\beta(\theta) = \frac{dI(\theta)}{EdV}, \tag{1}$$

For simplicity we omit the wavelength dependence of the VSF for the moment. We can express $dI(\theta)$ and E as $dI(\theta) = dF(\theta)/d\Omega$ and $E = F(\theta = 0)/dS$ where $F(\theta)$ is the scattered radiant flux (radiant energy per time) in the solid viewing angle of the detector, Ω, and $F(\theta = 0)$ is the radiant flux at the area of the scattering volume, dS, perpendicular to the incident beam. Since $dV = dSdz$ where z is an infinitesimal of the scattering volume, then Eq. (1) should be transformed into:

$$\beta(\theta) = \frac{1}{dzd\Omega}\frac{dF(\theta)}{F(\theta = 0)}, \tag{2}$$

As a result of the finite size of the scattering volume, the photo-sensor measures the scattered radiance $L(\theta)$, i.e. $L(\theta) = F(\theta)/dSd\Omega$. In the real experimental situation dV is surrounded by water. The flux in Eq. (2) can be replaced in terms of radiance, taking the attenuation of light into consideration;

#191692 - $15.00 USD Received 3 Jun 2013; revised 2 Jul 2013; accepted 8 Jul 2013; published 30 Jul 2013

$$\beta(\theta) = \frac{1}{dzd\Omega} \frac{L(\theta) e^{-c(l_1+l_2)}}{L'(\theta=0) e^{-c(l_1+l_2)}}, \tag{3}$$

where c is the total beam attenuation coefficient by water surrounding dV (m^{-1}), l_1 is the distance from the light source to the center of the scattering volume, and l_2 that between the center of the scattering volume and the detector (in meters). $L'(\theta = 0)$ represents the radiance observed far from the scattering volume at $\theta = 0$.

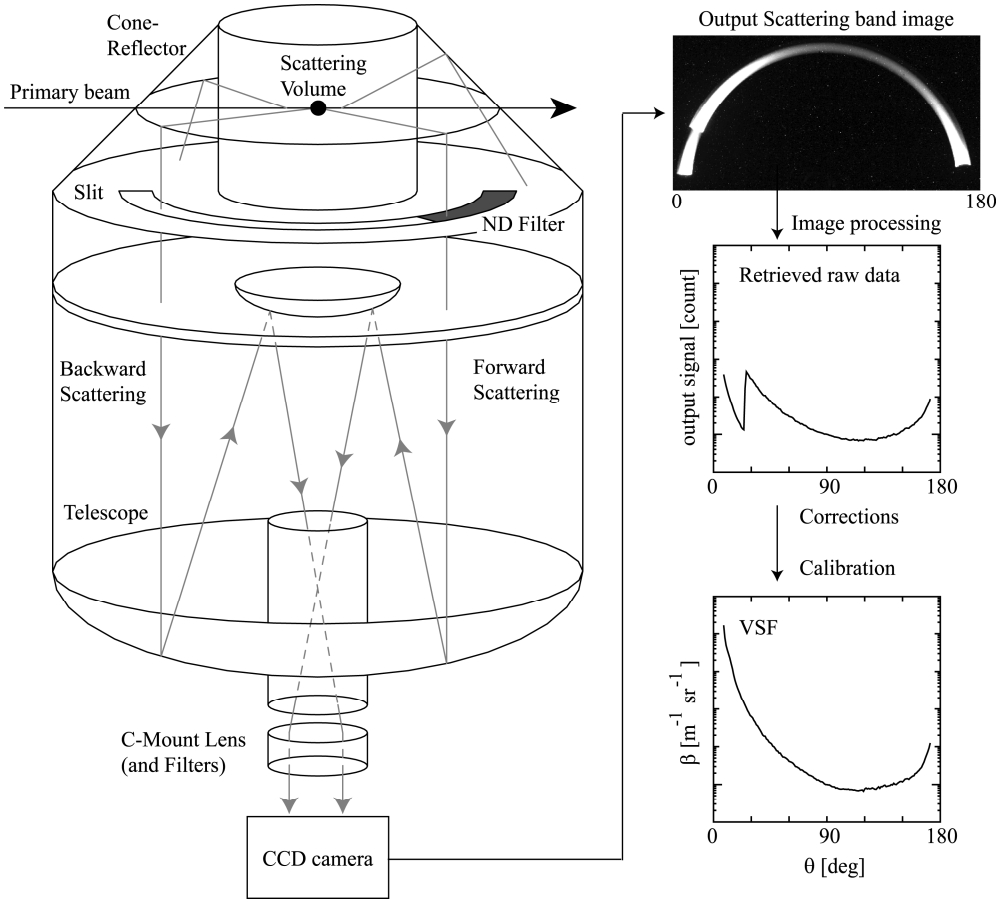

Fig. 1. A schematic representation of the measurement principle for VSF measurements by image detection based on the reflection system (left), as well as that of the data-flow for the retrieval of VSF from "output scattering band image" provided from the high sensitive CCD camera (right). Note that 1) the light source, the monochromator and the collimator were omitted from Fig. for convenience, and 2) the forward scattering (0°-25°) in the example photo-picture (left side of the photograph) is attenuated by the ND (Neutral Density) filter, that makes an mathematical adjustment necessary to retrieve the entire VSF.

General principle of the VSF instrument

The newly developed VSF meter equipped with an image detector, as shown in Fig. 1, applied a light reflection system that consists of a cone-reflector and a commercial telescope as the light collector. White light from a strong light source is turned into a collimated monochromatic light beam by a monochromator and a collimator. A cylindrical transparent glass container is placed in the center of the cone-reflector. A transparent conical flask that contains the sample is mounted in the center of this glass container, and surrounded by

#191692 - $15.00 USD Received 3 Jun 2013; revised 2 Jul 2013; accepted 8 Jul 2013; published 30 Jul 2013

purified water. The cone-reflector has an apex angle of 90° and reflects the horizontally scattered light from the light beam downwards and towards the telescope. An aluminum plate with a semicircular slit that is open over 180° is placed in front of the telescope's aperture to prevent the off-center scattered light from entering the telescope. The light detector, a high sensitivity air-cooled CCD camera, is placed at the focal point of the telescope. The detector captures the scattered light in form of a full image of the semi-circular slit.

The instrument has no moving parts and allows measurements of the VSF for angles between 8° and 172° at 1° intervals simultaneously at one wavelength within a few seconds. A spectral measurement from 400 nm to 700 nm (resolution 10- 20 nm) can be made in within 30 min by a manual wavelength scanning.

Specification and experimental setup

Light source

The light source is a plasma lamp unit (LIFI-INT-30-02, LUXIM Corp). As formulated in Eq. (1), the scattered intensity, or scattering signal, is proportional to the incoming irradiance energy upon the scattering volume. A Xenon arc lamp unit was often employed as light source for conventional VSF meters. Providing the radiation with electrical discharge (sparking), unfortunately, is accompanied by giving off flares that cause serious problems for scattering measurement. That is, 1) the variation of the radiant flux with time is subject to additional correction, which imposes measurement errors, 2) large variations in the radiant power over short time periods would have a strong impact upon the magnitude of output signal from the CCD camera especially when the integration time of the CCD camera is short. Deployment of the plasma lamp solved these problems since it provides an extremely stable (ca. 0.6% of the fluctuation on average for 2 hours) but still strong irradiance.

Monochromator and Collimator

A monochromator (SPG-120S, SHIMADZU) with an average FWHM (full width at the half of maximum) of ca. 15 nm was mounted between the plasma lamp and a custom-made collimator. The collimated beam has a diameter of 5 mm with 1° of divergence. Some field stops were placed inside the collimator and an absorptive black sheet was attached on the inside of the collimator to prevent undesired reflection.

Cone-reflector

The cone-reflector is made of 99.9% aluminum. The surface of the aluminum was well polished and coated with silica for anti-oxidation, and acts as a mirror. There are two drilled holes in the cone; one is for fixing in the collimator end, the other, on the opposite side of the cone, is open and acts as a light trap for the transmitted light from the primary beam.

Sample compartments

A custom-made glass container (DURAN, SCHOTT A.G.) is place in the center of the cone reflector and has the dimensions: outer diameter: 110.0 mm, wall thickness: 3.0 mm, height: 110.0 mm. In order to transmit the collimated primary beam perpendicularly to the scattering volume and then further on to the light trap, two quartz glass windows (10.0 mm of dia.) were fixed on two holes in the sample container by an optical bond, a flat one at the entrance side of the container and a sloped one at the exit side acting as a light trap. A normal or a commercial laboratory type VSF meter uses an optical light trap outside of the sample container for minimizing the reflection of the primary beam. However, this type light trap does not function to eliminate the reflected primary beam at the glass-air interface of the exit window. This becomes the constrain condition for measuring VSF in large scattering angle. By mounting a custom made light trap at the exit window, i.e., a 5° sloped quartz glass window bonded with 99.0% absorptive ND filter, we solve these problems: This light trap

#191692 - $15.00 USD Received 3 Jun 2013; revised 2 Jul 2013; accepted 8 Jul 2013; published 30 Jul 2013

reflects 0.4% of the primary beam at the sloped water-glass interface but this then penetrates through the sample cavity in an upward direction away from the detector side. Further, the ND filter then absorbs the primary beam passing through the slope window. The reflected light of the primary beam from the ND filter-air boundary returning toward the sample container is absorbed again by the ND filter. Finally, only 0.01% of the primary beam is reflected back into the sample container. In addition to the light trap, the slope of the triangular shaped sample flask also helps to divert reflections of the primary beam off-axis. Figure 2 shows a schematic diagram of the sample container with the light trap showing the reflection behavior of the primary beam. Given that the energy of forward scattering is significantly greater than that of backscattering, it is essential that reflections of forward scattered light are prevented from heading towards camera pixels measuring backscattering. Black tape was placed on the sample container wall to reduce these reflections, except for the side of scattering observation.

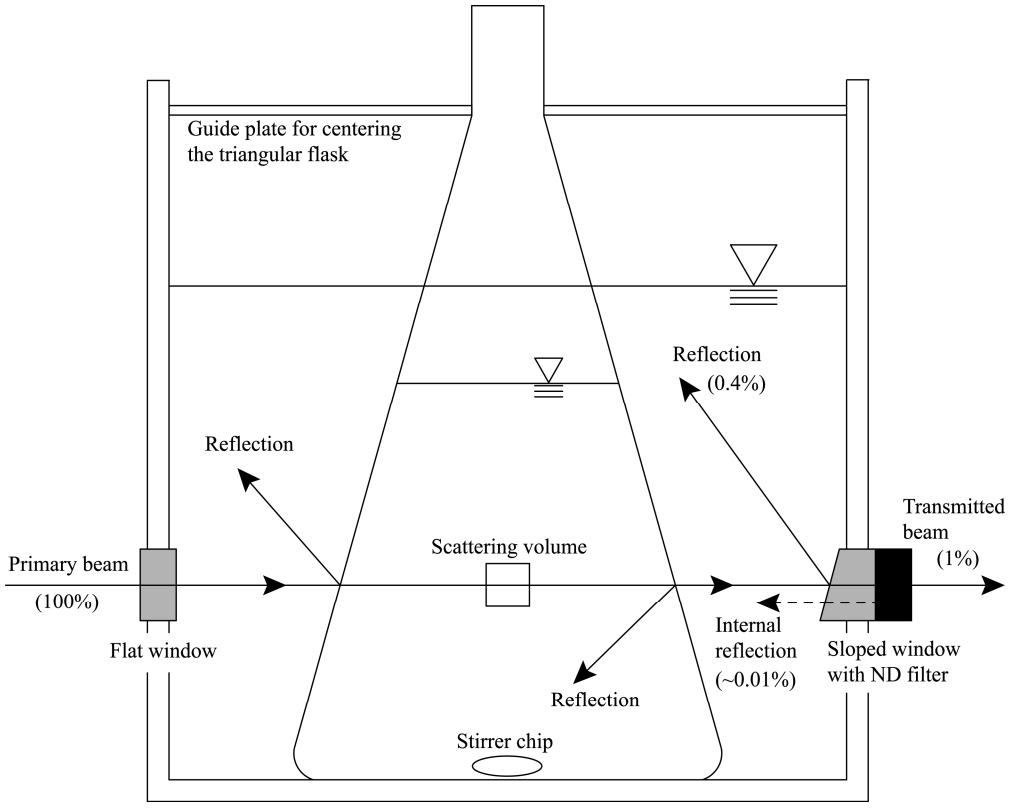

Fig. 2. A schematic diagram of the different pathways of the primary beam fractions, and of the construction of the sample container and the light trap designed to solve the problem of re-irradiation of the scattering volume with reflections of the primary beam. The percentage values in the parenthesis mean the radiant energy relative to the incoming primary beam.

Slit

The slit consists of a 180° semi-circular aperture (7 mm wide, diameter at the center of the aperture: 141.0 mm) in a round aluminum plate. The plate was painted black to reduce reflections. The dynamic range of the camera had to be adjusted to the large dynamic range of the signal across the circular slit. The intensity distribution along the slit represents scattering intensities over all angles. The strong signal from forward scattering was therefore attenuated by a thin film absorptive ND filter with ca. 1.5% transmittance (FUJI FILM Corp. ND1.8,

#191692 - $15.00 USD Received 3 Jun 2013; revised 2 Jul 2013; accepted 8 Jul 2013; published 30 Jul 2013

TF007M) that covered the slit from 0° to 25°. As a result, the VSF can be determined with the same integration time of the CCD camera in a single snapshot of the image.

Telescope

The telescope used is a Schmidt-Cassegrain (LX-90-SC, MEADE) with an aperture of 203 mm and a focal length of 2034 mm. The telescope consists of two spherical mirrors with "MEADE ultra-high transmission coatings" and a Schmidt correcting plate. The transmission of the telescope is over ca. 85% through the visible spectrum but declines slightly between 450 and 400 nm.

Detector

The detector-camera (ML77, Finger Lakes Instrumentation) has a back illuminated CCD chip (CCD77-00, Marconi), which has 24 μm pixels, 512 by 512 array size, and 16-bit digitization without anti-blooming structures to maximize the dynamic range. The CCD chip is cooled by thermoelectric cooling system without water assist, typical minimum temperature of –60°C with 0.1°C of stability. The image is obtained using data acquisition software, FLI Grab, via USB2.0. In order to retain the high-resolution image with the highest possible sensitivity, a fixed C-Mount lens (1A1HB, TAMRON corp.) is mounted on the CCD camera to achieve a state of fully opened aperture. A beam expander (NT54-357, Edmund Opt.) is also attached between the C-Mount lens and the CCD camera. During measurements of cultured phytoplankton at wavelengths below 480 nm, an optical short-pass filter that only transmitted light less than ca. 480 nm was attached to the C-Mount lens to absorb chlorophyll-a fluorescence (at ~680 nm) induced by the light during the VSF measurement.

Experimental setup

Before VSF measurements, the sample container and the triangular flask were well flushed several times with purified water. The CCD camera was cooled to −20°C to minimize signal noise. The sample was filled into the flask and the surrounding container filled with purified water. The sample was slowly stirred with the help of a magnetic stirrer to prevent sinking of particles without building up of bubbles [12, 19]. Purified water for surrounding the sample was prepared one day before and adapted to the room temperature. Experiments were started with a reference measurement for 400 to 480 nm with a fixed integration time of 120 sec and the short-pass filter in place. Then VSF measurements for these shorter wavelengths were carried out to search for an adequate integration time for each wavelength that did not saturate the detector. Afterwards the short pass filter was removed, and the same procedure conducted for wavelengths >480 nm. Finally, dark images were collected with the same integration times used for all VSF measurements.

3. Image processing, corrections and calibration

Image Processing

An image of the slit that includes the information of the angular distribution of the scattering signal is provided by the CCD camera in the FITS (Flexible Image Transport System) data format. This format contains an implicit pixel coordinate system of XY and depth values. To yield a dark corrected "scattering image", first, the image of the dark noise was subtracted from the raw "scattering image", and second, pixels outside the slit on the image (see Fig. 1) were use for an additional dark correction. These pixels represent an additional noise offset. A mean signal offset of the dark corrected image was calculated from 100-pixels outside of the slit image and additionally subtracted from the dark corrected image. To increase the signal-to-noise ratio, a binning of the scattering signal was performed: therefore the signal was summed up across the slit for each angle, using a circular mask with an appropriate size. The VSF in forward scattering by natural water or phytoplankton with broad size distribution is a

#191692 - $15.00 USD Received 3 Jun 2013; revised 2 Jul 2013; accepted 8 Jul 2013; published 30 Jul 2013

relative smooth function [8, 17, 21, 22]. Based on this fact, the entire scattering function was obtained by connecting the ND-filtered reduced signals with non ND-filtered signals by multiplying a constant factor. The proportional constant is the ratio at scattering angle 25° between the ND-attenuated signal and the non-attenuated extrapolated signal measured from 26° to 172° on logarithmic scale.

Integration time correction

As the integration time of the camera used for VSF measurements varied between 0.1 to 120 seconds, the linearity between the integration time and the output signal had to be experimentally validated. Therefore the camera was pointed to and focused on a white board from a distant of 650 mm. The board was illuminated uniformly by a halogen lamp. The output signal was set to be 55,000 counts for an integration time of 120 sec by changing the brightness of the halogen lamp. The integration time was then stepwise reduced to 0.1 sec and images collected for each step. A quadratic area of 100 by 100 pixels at the center of the collected images was chosen and the mean output value over the pixels in this area for each image calculated. The result showed that the camera possessed a very good linearity of the signal over the integration times (data not shown), and that the shutter speed corresponded well to the integration time of the camera. To correct for variations in the integration time during different experiments and measurements, the output signal was scaled to an integration time at 120 sec by multiplying a proportional constant of (120/T), in which T is the integration time of given VSF measurement in seconds.

Scattering volume correction

The scattering volume can be expressed as the volume illuminated by the incident beam per pixel and must be constant over all scattering angles to obtain the correct VSF. However, the volume varies in complex fashion as a function of the scattering angle due to the measurement principle. In an ideal case, the variation of the scattering volume relative to the scattering volume at 90° can be expressed as the inverse of a sine function when an incident beam and a receiver both have perfect parallel viewing geometries. This assumption is not satisfied in reality. Reasons for this are the divergence of the incident beam and variation in the acceptance angle for each pixel of the detector. To correct for these variations, an empirical function for correction of the scattering volume variation must be found. The angular distribution of fluorescence in solution is isotropic over all scattering angles [9]. Hence, the angular distribution of the output signal for fluorescent matter can be used to determine the instrument-specific variation of the scattering volume with scattering angle. The scattering function of a fluorescent dye, Fluoroscein (maximum excitation: 494 nm, maximum emission: 521 nm), dissolved in purified water was observed at 494 nm using an interference filter. The interference filter (central waveband is 580 nm) was placed in front of the camera to detect the fluorescence emission only. It should be noted that the output signal is not only a function of the variation of the scattering volume but also of the variation of the reflectance by reflectors over the scattering angles. The scattering volume variation was corrected by multiplying the measurements with the inverse of the scattering function of Fluoroscein for each scattering angle.

Attenuation correction

The attenuation coefficient of each sample was measured with a standard beam-transmission meter setup [23] in order to correct for attenuation of the primary beam and that of the scattered light while traversing through the sample. The transmission meter assembly consists of a collimator with the divergence angle of 0.11° and a hyper-spectral detector (RAMSES-ARC, TRIOS GmbH, Germany) with the lens-pinhole system of which the acceptance angle is 0.85°. Light from a plasma lamp was guided by an optical fiber (0.2 μm dia.) to the collimator before passing through a glass cuvette with an optical path length of 150.0 mm.

#191692 - $15.00 USD Received 3 Jun 2013; revised 2 Jul 2013; accepted 8 Jul 2013; published 30 Jul 2013

Freshly purified water was used as a reference. The influence of multiple reflections at the physical boundaries of glass and/or air to water due to the refractive index differences were neglected but for most wavelength were negligible. As freshly purified water was used as a reference, the total beam attenuation coefficient is calculated by summing up the total absorption coefficient [24] and the total scattering coefficient of pure water [25] to the measured beam attenuation coefficient. Note that light scattered at forward angles less than 0.85° was detected, resulting in underestimating the attenuation. Because of the instrumental design and calibration procedure (explained below), we assumed that l_1 and l_2 in Eq. (3) are equal. Since the sample is surrounded by purified water, the total length of l_1 and l_2 was interpreted as being equal to the mean central diameter of the triangle flask where the primary beam penetrates through. In this study, 0.0775 m was used for the final attenuation correction.

Calibration

The output signal was calibrated by measuring the absolute magnitude of VSF in $m^{-1}sr^{-1}$ of a standard solution for which the scattering magnitude is known. Spectroscopically pure methanol (WAKO Pure Chemical ind.) was employed for this calibration for the following reasons: 1) the refractive index of methanol is close to that of water. It is therefore not necessary to additionally correct for the scattering volume variations and for the specular reflections at physical boundaries induced by refractive index differences between water and methanol, 2) for the entire visible spectrum methanol has a high scattering coefficient, more than two times that of pure water, and 3) the production of optically pure water, i.e. without any particulate matter or bubbles, is difficult. The absolute values of scattering by methanol in the visible domain (400 to 700 nm) was adopted from Oishi [21].

4. Assessment of the instrument

We first present VSF measurements of purified water as a representative for molecular scattering and compare with the theoretically calculated VSF of optically pure water [25]. The spectral measurement for purified water was conducted with a fixed integration time of 120 sec for 400 to 680 nm in 20 nm intervals. Figure 3 shows the measured spectral scattering coefficient at 90° together with a theoretical function. The measured scattering is very similar to the theoretical values except in the red part of spectrum where a maximum difference of 30% is found. A reason for these stronger differences could be poor signal-to-noise ratio at wavelengths with low scattering.

Purified water is an extreme medium possessing the lowest VSF we shall deal with in this paper. An accuracy of VSF measurement can be determined by summation of measurement errors by purified water, by methanol, and the uncertainty of the Rayleigh ratio of methanol, $\beta_m(90)$. 20 measurements of purified water and methanol at 550 nm were carried out. Note that the error due to the intensity fluctuation of the plasma lamp unit is involved in these measurements. The Rayleigh ratio of purified water, $\beta_w(90)$, in absolute values was obtained by the output signal of water and of methanol, $S_w(90)$ and $S_m(90)$, respectively, as following;

$$\beta_w(90) = \beta_m(90)\frac{S_w(90)}{S_m(90)}, \tag{4}$$

So that the accuracy of $\beta_w(90)$ is estimated from:

$$\left|\frac{\Delta\beta_w(90)}{\beta_w(90)}\right| \le \left|\frac{\Delta\beta_m(90)}{\beta_m(90)}\right| + \left|\frac{\Delta S_w(90)}{A_w(90)}\right| + \left|\frac{\Delta S_m(90)}{A_m(90)}\right|, \tag{5}$$

where $A_{w,m}(90)$ and $\Delta S_{w,m}(90)$ are the averages and the deviations of the output signals of purified water and of methanol, respectively. The instrument gives 15% errors for VSF measurements.

#191692 - $15.00 USD Received 3 Jun 2013; revised 2 Jul 2013; accepted 8 Jul 2013; published 30 Jul 2013

Further validation was obtained with VSF measurement on standard particle. Non-absorbing spherically uniform polymer micro-particle of Latex was used for this purpose. The Latex particle (Duke Scientific Corp.) had mean diameter of 10.9 ± 0.3 μm (s.e. of mean) with a standard deviation of 1.0 μm with respect to the particle size distribution and a refractive index of 1.20 (relative to water) at 589 nm. With these parameters, the theoretical scattering function was computed with Lorentz-Mie scattering theory (e.g [22].) assuming a Gaussian particle size distribution. The VSF experiment was conducted by suspending the Latex particles in purified water. Figure 4 presents normalized VSF at 550 nm for particle together with normalized theoretically determined scattering function for comparison. The result showed that the VSF is very similar to the predicted one in the following respects: the straight increase at forward scattering angle on the logarithmic scale, the appearance of peaks at around 120° as well as 130°, and the gradual escalation after 150°.

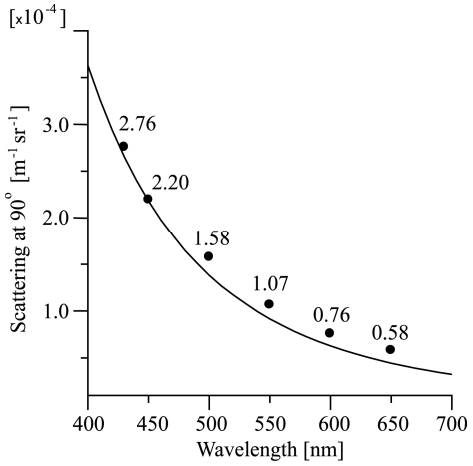

Fig. 3. Comparison of spectral scattering at 90° in absolute unit between theoretical value (solid line) of optically pure water by Morel (1974) and direct measurements (symbols) of purified water. It should be noted that measurements at 400 nm and 700 nm were omitted due to the poor signal-to-noise ratio.

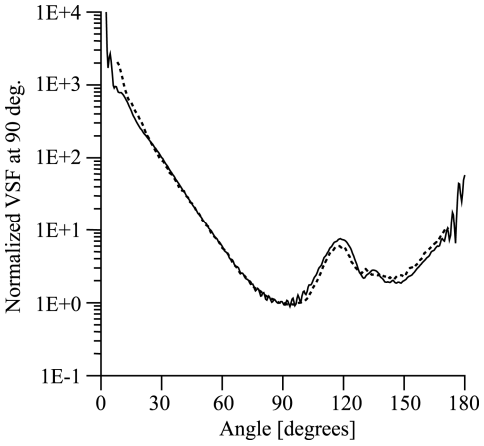

Fig. 4. Normalized VSF of direct measurement (dashed line) at 550 nm for Latex particle with mean diameter of 10.9 μm. For comparison theoretically calculated functions (solid line) are shown. Note that 1E-1 is 10^{-1} on ordinate.

#191692 - $15.00 USD Received 3 Jun 2013; revised 2 Jul 2013; accepted 8 Jul 2013; published 30 Jul 2013

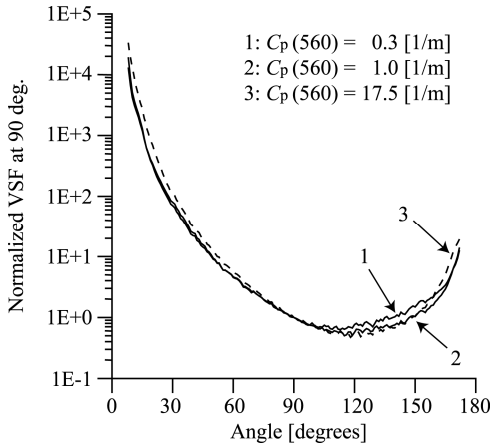

Fig. 5. Comparison with the VSF shape in different concentrations. (Sample: *Nannochloropsis sp.* at 560 nm). The VSF with the maximum c_p in this study is indicated as dashed line.

It is also important to assess the effects of multiple scattering to the determination of the VSF. Phenomenologically and theoretically, for example the extended Hartel theory [26], the modification of VSF with respect to its shape appears most significantly in forward scattering direction (if the influence of multiple scattering is not negligible on the VSF measurement). We made additional experiments to investigate the constancy of the VSF shape as a function of particle attenuation, c_p. As shown in Fig. 5, the shapes of the VSF are fairly similar to each other not only in general angles but also in small forward angles even when the attenuation is varied over almost 2 orders of magnitude.

Judging from the above results it is concluded that 1) suspicious peaks due to any unexpected instrumental specular reflections were not observed, thus the reflections at physical boundaries do not artificially influence the VSF measurement, up to large scattering angle, 2) the instrument gives a reliable VSF result even when the attenuation is high (up to 17.5 [1/m]). These imply that the light traps mounted on the sample container, all corrections and calibration work properly. and 3) the instrument determines the VSF within a few seconds from 8° to 172° with sufficient angular resolution of 1° without the need to change the sensitivity of the detector.

5. VSF variability for cultured phytoplankton

Spectral VSF measurements were carried out with five species of cultured phytoplanktonic algae, i.e. with cells of the dinoflagellate *Prorocentrum minimum* (Pavillard) Schiller, of the marine flagellate *Rhodomonas balthica* Karsten, of a blue-green algae *Synechococcus sp.*, of the green algae *Nannochloropsis sp.*, and of the centric diatom *Thalassiosira weissflogii* (Grunow) G.Fryxell & Hasle. Cultures were provided by the Alfred-Wegener Institute for Polar and Marine Research, were grown in F/2 medium under 12 h of light, and collected during their exponential growth phase. According to the encyclopedia of phytoplankton [27] and that on web [28], these species have different size and form parameters: *P. minimum* has a triaxial ellipsoid (triangular to oval and to heart) shape with 14-22 μm of diameter and 10-15 μm of length. *R. baltica* was colored red or red-brown and has a ovoid shape with cell sizes ca. 10-30 μm. *Synechococcus* sp. is a picoplankton species, its spherical shape varies from ca. 0.8 to 1.5 μm. *Nannochloropsis* sp. is also small, approximately 2 μm with a spherical shape. The microalgae *T. weissflogii* has a short cylindrical shape with sizes between 4 and 32 μm. Their particle diameters were determined by flow-cytometer (Cytobuoy, Cytosense) (see Table 1). Just before VSF measurement, they were diluted with F/2 medium filtered with the membrane filter of 0.22 μm pore size. Finally, Particulate VSF is obtained by subtracting VSF of seawater (35‰) from the measured VSF [22].

#191692 - $15.00 USD Received 3 Jun 2013; revised 2 Jul 2013; accepted 8 Jul 2013; published 30 Jul 2013

Table 1. Mean size and shape for five species of cultured phytoplankton

Cultures	Dia. [μm]	Shape
P. minimum	15.8	Ellipsoid
R. balthica	12.6	Ovoid
Synechococcus sp.	12.6	Spherical
Nannochloropsis sp.	15.8	Spherical
T. weissflogii	19.9	Cylindrical

Figure 6 illustrates the degree of spectral shape variations of VSFs for all cultured algae. The mean VSF shape derived from all measured wavelengths (normalized at 90°), and that of one standard deviation are shown. Differences in the features of VSFs of different cultured phytoplankton appeared in terms of: 1) the steepness at forward angle less than 30°, 2) the flatness over 90° to 150°, 3) the diversity after 150° and 4) the occurrences of spectral variance at around 50° and 120°. Focusing on the mean VSF shape difference, the VSF for *P. minimum* and *T. weissflogii* are similar with respect to the relatively small forward and backward scattering. Whereas VSFs for *R. balthica* and *Nannochloropsis sp.* showed pronounced forward as well as backward scattering, significantly more intense, by a factor of 1.5 to 3, compared to the others. While the VSF for *Synechococcus sp.* from 15° to 160° is similar to that of *R. balthica*, the VSF at less than 160° is almost coincident with those of *P. minimum*. From the cell shape viewpoint, *Synechococcus sp.* and *Nannochloropsis sp.* are spherical, so these as well as the ovoid shape of *R. balthica* can likely be treated as spheres. *P. minimum* and *T. weissflogii*, on the other hand, have entirely different cell shapes. The variability around 50° and 120° could be explained by the rainbow effect [29], for which the angle of appearance is related to the internal structure and refractive indices of scattering particles. Measured particle size distributions for the samples, i.e. monospecific cultured phytoplankton, followed the pattern of a Gaussian (normal) distribution; in this case, the VSF could form a noticeable peak or peaks if the particle was relatively large and transparent. The emerging angle(s) transits to forward direction when the refractive index relative to water is close to 1.0 [22], e.g. appeared around 120° and 130° for Latex particles (see Fig. 4). For phytoplankton, assuming a relative refractive index of ca. 1.06 [30, 31], the peaks appear at approximately 60° and 120°, when computed via Mie theory using measured particle size distributions and assuming absorptive particles (Figs. not shown).

#191692 - $15.00 USD Received 3 Jun 2013; revised 2 Jul 2013; accepted 8 Jul 2013; published 30 Jul 2013

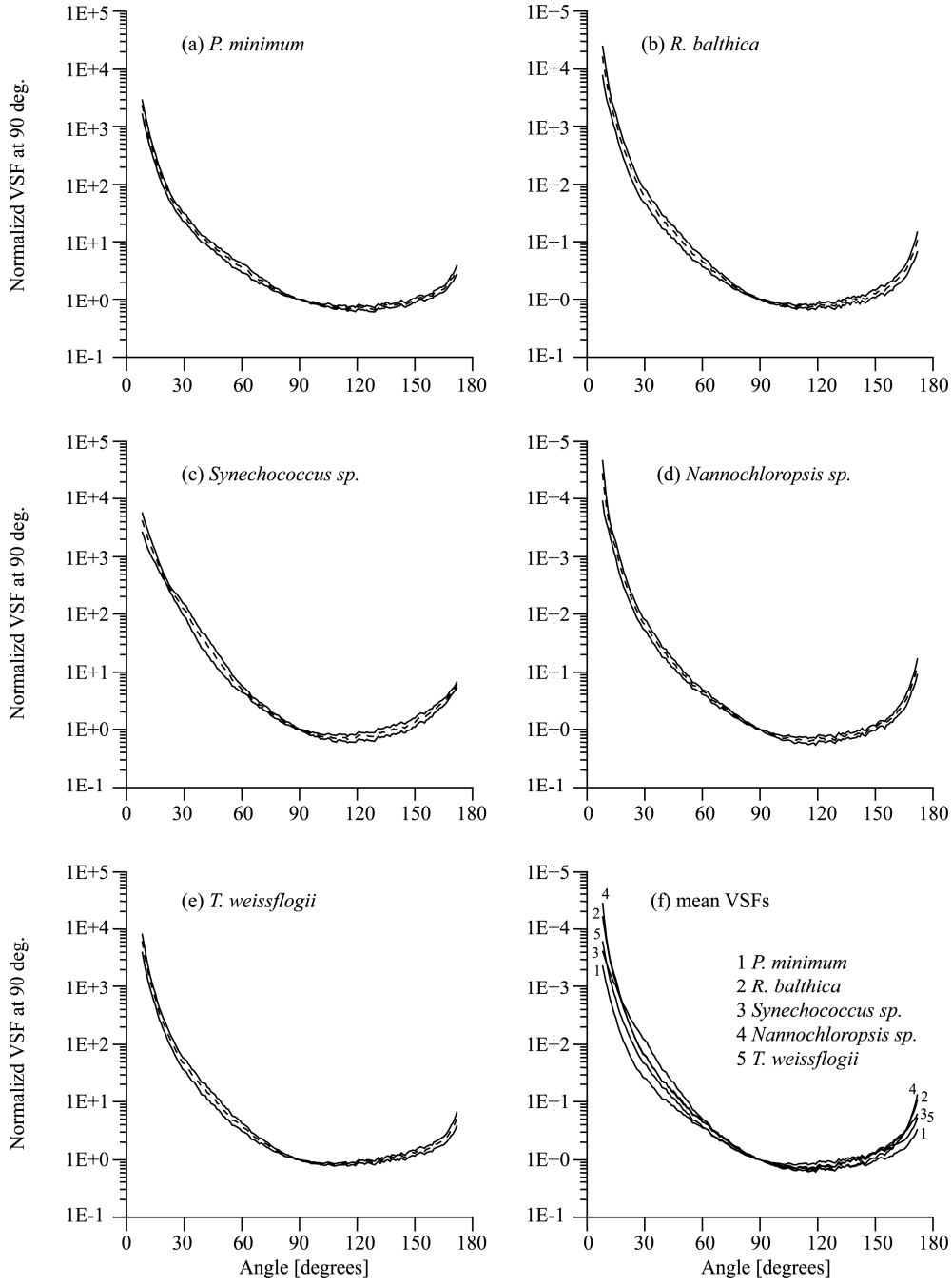

Fig. 6. Spectral variation and mean of VSFs for different algal species, (a) to (e) with one standard deviation (dot), (f) comparison among mean VSFs for all cultures. Mean VSF and one standard deviation were determined through all wavelengths: width between the solid lines is associated with the degree of spectral dependency. Note that 1E-1 is 10^{-1} on ordinate.

The measurements allow a fast determination of the VSF at different wavelength with a rather higher spectral resolution. Figure 7 shows the spectral scattering coefficient at selected scattering angles (10°, 30°, 60°, 90°, 120° and 170° respectively) in absolute values for *P. minimum* and *Synechococcus sp*. As a common feature at all backward angles except 170°,

#191692 - $15.00 USD Received 3 Jun 2013; revised 2 Jul 2013; accepted 8 Jul 2013; published 30 Jul 2013

the scattering coefficient was depressed around 460 nm, i.e. at a slightly longer wavelength than that of the strong absorption peaks. For *P. minimum* a trough at 670 nm not only for backward but also for forward angles was observed, whereas for *Synechococcus sp*. such a trough did not appear. Spectra in forward angles as well as at 170° are almost constant or slightly decrease toward red part of the spectrum without clear spectral features, except for *P. minimum* at 60°. The VSF is likely to depend on phytoplankton species with respect to the degree and the angle of trough: a strong variance of the shape of the VSF for different species and a strong variance of the spectral behavior with pronounced common spectral features in the near forward and backward directions. In particular backscattering differed strongly for different phytoplankton species. Differences of these phytoplankton species with respect to particle size, shape, internal structure, inhomogeneity, and refractive index will have a strong influence on the amount of light scattering (e.g [32, 33].), in particular backward scattering (e.g [34, 35].).

Stramski et al. [36] have pointed out that modeling backscattering from marine particles with their complex shape using Mie computation is a very difficult task. Zhou et al. [37] have demonstrated that the spectral property of backscattering strongly covaried with the absorption spectrum through anomalous dispersion in the refractive index. The features observed here can be explained by anomalous dispersion but seem to be less pronounced compared to the results of Zhou et al [37]. As we did not eliminate the influence of chlorophyll fluorescence at wavelengths >500 nm, small artifacts can be expected here, precluding a final conclusion about the wavelength dependence of the VSF at these longer wavelengths

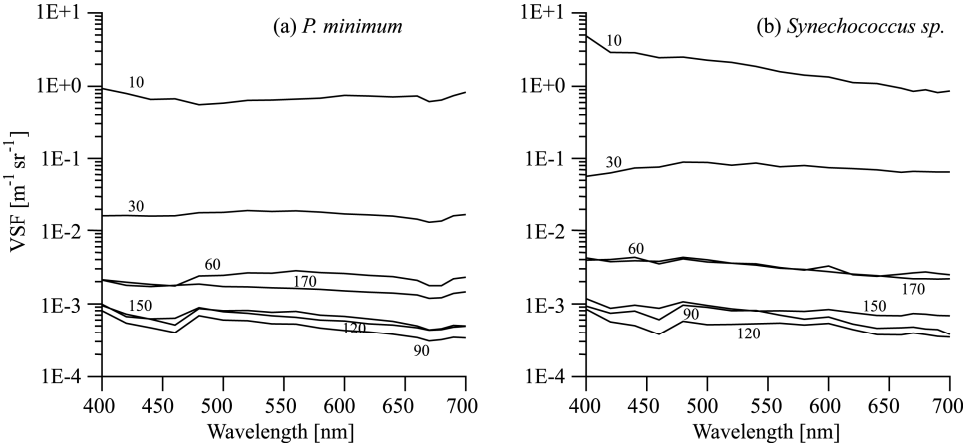

Fig. 7. Wavelength dependence of scattering coefficient at selected angles for (a) *P. minimum* and (b) *Synechococcus sp*. The numbers superimposed on graphs represent the scattering angle.

6. Conclusion

In this study, we developed a new volume scattering function (VSF) meter. With the unique measurement principle and the high sensitive CCD image sensor, the instrument is capable of the simultaneous capturing an image that is directly related to the angular distribution of scattering at 8° to 172° without changing the sensitivity of the detector and without having any moving optical parts, and can do so within a practical time in swift. In addition it allows fast spectral measurements with a high spectral resolution over the visible range. As a result of deploying the new custom light trap, based upon the absorptive ND filter with tilted glass window as well as the sample flask with triangular shape, it can eliminate functionally the re-irradiation of the scattering volume with the reflections of the primary beam from physical boundaries. Therefore any corrections are not necessary, and measured VSFs, even for large

#191692 - $15.00 USD Received 3 Jun 2013; revised 2 Jul 2013; accepted 8 Jul 2013; published 30 Jul 2013

scattering angles, are negligibly affected by the artificial reflections, which is one of the critical issues for assessing the VSF in laboratory measurements. The validation of the instrument under controlled conditions using scattering of standard liquids and particle suspensions agreed well with theoretically estimated functions for both molecular and particulate scattering cases.

With some further improvements (e.g. chlorophyll fluorescence correction at longer wavelength, better CCD camera, stronger light source) the instrument will allow relatively fast investigation of the VSF of different kinds of particle suspensions in samples from natural oceanic waters, especially from coastal waters, and from more phytoplankton species, including some special particle types such as calcareous coccoliths. For these investigations accurate data of the following complementary properties are required: absorption, attenuation, particle shape and particle size distribution, pigments concentration, and the refractive index. For phytoplankton cells it will be interesting to examine to what degree the growth conditions (e.g. light, temperature, salinity and nutrition) influence the VSF characteristics. The newly developed VSF meter for laboratory measurement can surely help with the routine work of collecting the VSF for marine particles including their spectral property that is one of the most lacked data in ocean optics. Accurate and easily obtained VSF measurements will improve radiation transfer modeling and optical remote sensing applications.

Acknowledgment

This study was supported by German Academic Exchange Service (Deutscher Akademischer Austauschdienst, DAAD). We thank David McKee, Hajo Krasemann, and Rüdiger Röttgers for comments on the paper. Our cordial thanks go to reviewers for improving the article.

#191692 - $15.00 USD Received 3 Jun 2013; revised 2 Jul 2013; accepted 8 Jul 2013; published 30 Jul 2013